Development of an Electron-Tracking Compton Camera using CF_4 gas at high pressure for improved detection efficiency

Michiaki Takahashi[a], Shigeto Kabuki[a], Kaori Hattori[a], Naoki Higashi[a], Satoru Iwaki[a], Hidetoshi Kubo[a], Shunsuke Kurosawa[a], Kentaro Miuchi[a], Keseki Nakamura[a], Hironobu Nishimura[a], Joseph D. Parker[a], Tatsuya Sawano[a], Atsushi Takada[b], Toru Tanimori[a], Kojiro Taniue[a], Kazuki Ueno[a]

[a]*Department of Physics, Graduate School of Science, Kyoto University, Kitashirakawa, Sakyo, Kyoto 606-8502, Japan*
[b]*Scientific Balloon Laboratory, ISAS, JAXA and Yoshinodai, Sagamihara, Kanagawa 229-8510, Japan*

Abstract

We have developed an Electron-Tracking Compton Camera (ETCC) for medical imaging and MeV gamma-ray astronomy. The ETCC consists of a gaseous Time Projection Chamber (μTPC) and pixel scintillator arrays. To improve the detection efficiency, we have optimized the gas mixture in the μTPC and operated the ETCC at high pressure. Basic characteristics such as the gas gain, drift velocity, energy resolution, and position resolution of the μTPC were examined, and using this optimization, both the efficiency and the angular resolution of the ETCC were measured. We achieved a steady gas gain of $\sim$ 20,000 in $Ar/CF_4/isoC_4H_{10}$ (54:40:6) at 1.4 atm. The diffusion constant in $Ar/CF_4/isoC_4H_{10}$ (54:40:6) at 1.4 atm was $\sim$ 2 times better than in Ar/C_2H_6 (90:10) at 1 atm. The efficiency in $Ar/CF_4/isoC_4H_{10}$ (54:40:6) at 1.4 atm was also $\sim$ 2 times higher than in Ar/C_2H_6 (90:10) at 1 atm.

Key words: Gaseous detector, CF_4, Time projection chamber, Compton imaging, μPIC, GEM

1. Introduction

For medical imaging and MeV gamma-ray astronomy, we have developed an Electron-Tracking Compton Camera (ETCC). A schematic view of the ETCC is shown in Figure 1(a). The ETCC uses Compton scattering to detect MeV gamma rays, and consists of a gaseous micro Time Projection Chamber (μTPC) and Pixel Scintillator Arrays (PSAs) surrounding the μTPC [1]. In order to measure the direction and energy of the Compton-recoil electron, we use the μTPC based on a Gas Electron Multiplier (GEM [2]) and a micro-PIxel Chamber (μPIC [3]). The position and energy of the Compton scattered gamma ray is measured by the PSA. Thus, the ETCC is able to reconstruct the direction and energy for a single photon.

The μTPC consists of a drift cage, a GEM, and a μPIC. A schematic view of the μTPC is shown in Figure 1(b). A recoil electron ionizes the gas along its track, producing electrons. These electrons drift toward the μPIC along the electric field in the drift cage and are then amplified by the GEM and the μPIC. The μPIC is a gaseous two-dimensional position-sensitive detector manufactured in printed circuit board technology. Since anode and cathode strips are arranged perpendicular to each other, a two-dimensional readout is available. The detection area of the μPIC is 10×10 cm^2 and the pixel pitch is 400 μm. The one-dimensional position resolution of the μPIC is $\sim$ 120 μm. The μPIC has achieved a maximum gas gain of 16,000 and has been stably operated at a gas gain of 6000 for more than 1000 hours. In order to maintain stable operation, the gas gain of the μPIC has been reduced to 3000. The GEM was used as a supplementary multiplier, and was operated with a gain of about 10. Several prototype μTPCs with a detection volume of about $10\times10\times10$ cm^3 filled with an Ar/C_2H_6 (90:10) gas mixture at 1 atm were developed, and their performances were already reported [4].

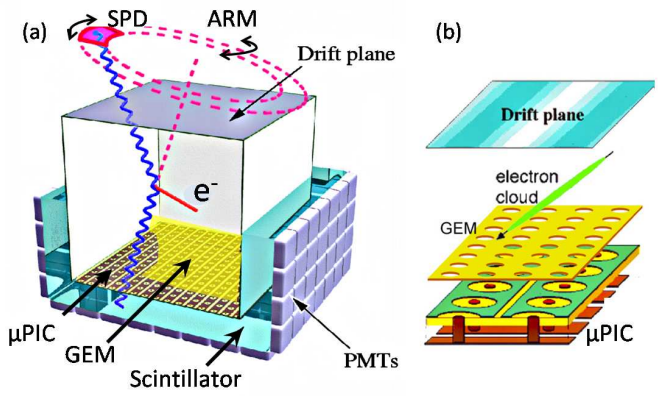

Figure 1: (a) Schematic view of the ETCC consisting of a μTPC and PSAs; and (b) Schematic view of the μTPC consisting of a drift cage, a GEM, and a μPIC.

For the scintillators in the PSAs, we have used GSO:Ce or $LaBr_3$:Ce scintillators [5]. We made scintillator pixels with a size of $6 \times 6 \times 13$ mm^3, and assembled them into 8×8 pixel arrays. One camera consists of 9 such arrays. For the scintillators' photon sensors, we selected a multi-anode photomultiplier (Hamamatsu Photonics Flat-Panel H8500) which consists of dynodes of a size of 6×6 mm^2 arranged in an 8×8 array [6]. To reduce the number of readout channels, chained resistors were used, and we obtained the position of a hit pixel by the

charge-division method [7]. The energy resolution of $LaBr_3$:Ce is better than that of the GSO:Ce scintillator. The Full Width at Half Maximum (FWHM) of the energy resolution for a GSO:Ce PSA is 10.4% at 662 keV, while that of a $LaBr_3$:Ce PSA is 5.8% at 662 keV [8].

The angular resolution of the ETCC is defined by two parameters: the Angular Resolution Measure (ARM) which indicates the accuracy of the scattering angle, and the Scatter Plane Deviation (SPD) which represents the accuracy of the determination of the Compton-scattering plane as shown in Figure 1(a). The best record of our prototype is about 7° (FWHM of the ARM at 662 keV).

The ETCC has a wide energy dynamic range of 100-3000 keV (PET: 511 keV, SPECT: < 300 keV) and a wide field of view of ~ 3 sr, and hence for medical imaging, we could develop new RI drugs and perform multi-RI tracer imaging. We administered ^{65}Zn to mice and succeeded its imaging at 1116 keV in ~ 110 hours. We also administered two drugs (I-131-MIBG and F-18-FDG) to mice and realized double tracer imaging (356 keV and 511 keV, respectively) in ~ 6 hours [9].

The ETCC is also used for astronomy. We are planning a balloon experiment, known as Sub-MeV gamma-ray Imaging Loaded-on-balloon Experiment (SMILE). As the first step of SMILE, we launched an ETCC in 2006 [10]. In this flight, we successfully detected about 400 gamma-ray events in 3 hours. For the next step, we plan to launch a large ETCC to observe the Crab Nebula or Cygnus X-1.

Although our ETCC has a wide energy dynamic range, it has a poor sensitivity. Therefore, we have to improve the sensitivity.

2. Optimizing the gas mixture

2.1. Gas selection

For the optimization, CF_4 gas was chosen. There are two merits of CF_4 gas: 1) small diffusion of electrons, and 2) a large cross-section for Compton scattering. A small diffusion of electrons in the CF_4 gas provides both better position resolution for the μTPC and better angular resolution for the ETCC. The large cross section in Compton scattering is due to its 42 electrons in one molecule. The low-Z atoms also give us a small multiple scattering for the recoil electrons. This increases the efficiency for the ETCC. On the other hand, there are demerits. A little contamination of the CF_4 causes a low gas gain. To overcome this, we introduced $isoC_4H_{10}$ which has a low W value. In addition, the drift velocity of CF_4 strongly depends on the electric field. Thus a good uniformity of the electric field is needed in the μTPC.

2.2. Setup

The gas gain was measured in the prototype μTPC using 31 keV X-rays from ^{133}Ba. In this experiment, the 50-μm-thick GEM made of a polyimide insulator, and the GSO:Ce PSAs were used.

We used four gases (Ar/C_2H_6 (90:10), Ar, CF_4, and $isoC_4H_{10}$) in this study, we blended these gases, and examined 45 different varieties of blended gas.

2.3. Results

The measured charge distributions of the signals were fitted with a Gaussian. The amount of induced charge is obtained as the mean value of the fitted Gaussian function. The gas gain is obtained using the following equation:

$$\text{Gas Gain} = \frac{Q\ [\text{C}]}{e\ [\text{C}] \times (31 \times 10^3\ [\text{eV}]/W\ [\text{eV}]) \times A} \quad (1)$$

where W stands for the average energy to generate an electron-ion pair, e is the unit charge, Q is the measured charge, and A is the gain of the preamplifier. The value for W is 27 eV in C_2H_6, 54 eV in CF_4, 26 eV in Ar, and 23 eV in $isoC_4H_{10}$.

When we used $isoC_4H_{10}$, the gas gain improved by more than a factor of 2. The main results are shown in Figure 2. In this experiment, the voltage between the top and bottom surface of the GEM was 340 V in Ar/C_2H_6 (90:10), and 400 V for all other mixtures. We achieved a stable gas gain of about 20,000 in $Ar/CF_4/isoC_4H_{10}$ (54:40:6) at 1 atm.

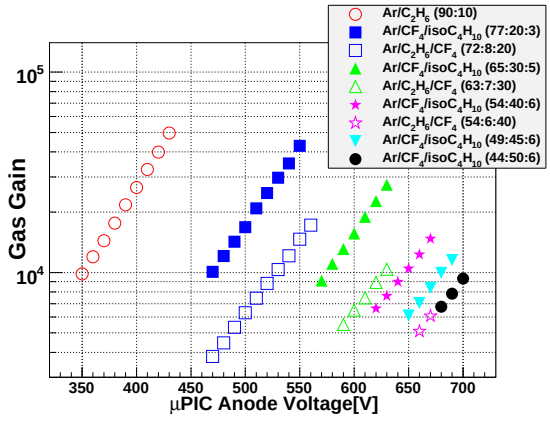

Figure 2: Gas gain as a function of the μPIC anode voltage.

3. Operation at high pressure

3.1. Setup

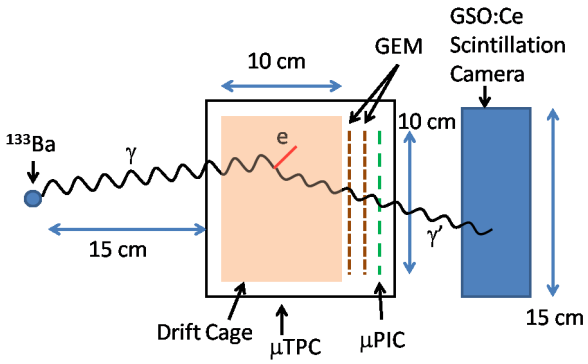

Figure 3: Schematic drawing of the experimental setup.

We operated the ETCC, shown in Figure 3, at high pressure. Since the gas gain is a function of E/P (E: electric field, P: gas pressure), the gas gain becomes lower at high pressure for the same E. Thus, to obtain adequate gain at high pressure, we used two GEMs in this experiment. Both GEMs are made of liquid crystal polymer [11], and the thicknesses of the upper and lower GEM are 100 μm and 50 μm, respectively. The lengths of the transfer and of the induction region are 2 mm each. The detection volume of the μTPC is $10 \times 10 \times 10$ cm^3. On the top of the drift cage, we put a cover made of aluminum whose thickness is 1 cm.

3.2. Performance of the μTPC

We used Ar/C_2H_6 (90:10) at 1 atm and at 2 atm, and Ar/CF_4/isoC$_4$H$_{10}$ (54:40:6) at 1 atm and 1.4 atm. We then compared the performances by measuring the gas gain, drift velocity, position resolution, and energy resolution of the μTPC for these four conditions.

The results of the gas gain measurements are shown in Figure 4. Here the gas gain becomes lower at high pressure.

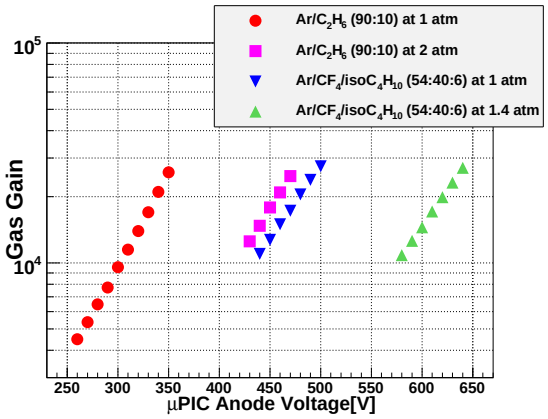

Figure 4: Gas gain as a function of the μPIC anode voltage.

In order to measure the drift velocity of electrons in the μTPC, GSO:Ce PSAs were placed at the back of the μTPC to serve as an event trigger. The drift velocity is obtained using the following relation:

$$\text{Drift Velocity} = \frac{l}{(\text{last clock} - \text{first clock})/100\ [\text{MHz}]}, \quad (2)$$

where l is the drift length, and first clock and last clock are the first-hit and the last-hit timing in a position encoder [12], respectively. We encode events with a 10 ns clock cycle. Figure 5 is the result of these drift velocity measurements. The difference between the simulation and the measurement is smaller than about 10%.

To estimate the position resolution of the μTPC using the tracks of cosmic muons, two plastic scintillators were placed at the top of the μTPC, and GSO:Ce PSAs were placed at the back of the μTPC. The coincidence of these scintillators was required. We fitted the hit points with a line and calculated the residual. We then fitted the distribution of the residual with

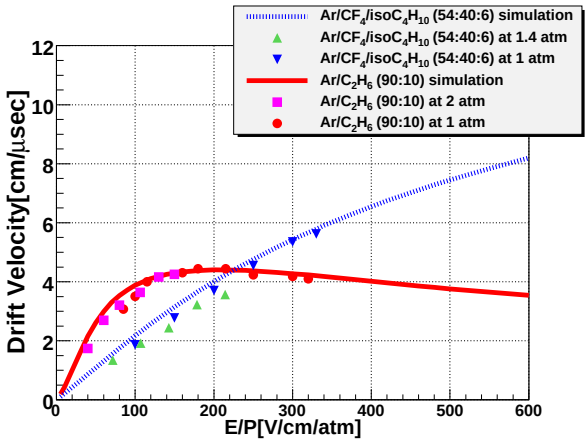

Figure 5: Drift velocity of electrons as a function of the reduced electric field (E/P). The lines are simulation results using Magboltz [13], and the data are shown as points.

a two-dimensional Gaussian curve. The standard deviation σ is the position resolution. We determined the position resolution for each 1 cm of the drift length from bottom to top. The figures 6 and 7 show the results of the position resolution measurements in Ar/C_2H_6 (90:10) at 1 atm, and in Ar/CF_4/isoC$_4$H$_{10}$ (54:40:6) at 1.4 atm, respectively. We fit these plots with

$$\sigma^2(l) = \sigma^2_{\text{detector}} + (D\sqrt{l})^2, \quad (3)$$

where $\sigma\,(0) = \sigma_{\text{detector}}$, and D is the diffusion constant. The one-dimensional position resolution is given by $\sigma_0 = \sigma_{\text{detector}} / \sqrt{2}$.

The diffusion constant for Ar/CF_4/isoC$_4$H$_{10}$ (54:40:6) at 1.4 atm is better by a factor of ~ 2 compared to Ar/C_2H_6 (90:10) at 1 atm. Here, Ar/CF_4/isoC$_4$H$_{10}$ (54:40:6) at 1.4 atm has a good position resolution. However, the one-dimensional position resolution at the bottom of the drift cage is worse than that of our prototypes. This may be attributed to the fact that the uniformity of the electric field in this μTPC might not be as good, compared to other μTPCs.

We also measured the energy resolution. The FWHM of the energy resolution was 43.8% for 31 keV which was worse by a factor of about 2 compared to our prototypes. This may also be attributed to the gain non-uniformity of the GEM in this μTPC.

High Voltage (HV) parameters of the GEMs, the position resolutions, and the diffusion constants are listed in Table 1.

3.3. Performance of the ETCC

We examined the performance of the ETCC using the μTPC. We used GSO:Ce PSAs in this experiment. We put ^{133}Ba (356 keV, 800 kBq) 15 cm away from the top of the μTPC and reconstructed the gamma rays (Figure 3). We measured the efficiency, ARM, and SPD of the ETCC, respectively. The operation gas gain of the ETCC was $\sim 2 \times 10^4$.

The results of this experiment are listed in Table 2. The efficiency with Ar/CF_4/isoC$_4$H$_{10}$ (54:40:6) at 1.4 atm was better by a factor of about 2 than with Ar/C_2H_6 (90:10) at 1 atm. For ARM and SPD, the results with Ar/CF_4/isoC$_4$H$_{10}$ (54:40:6) at

Table 1: HV parameters and results (upper GEM's top: HV1, upper GEM's bottom: HV2, lower GEM's top: HV3, and lower GEM's bottom: HV4)

Gas	Pressure	HV1	HV2	HV3	HV4	σ_0	D
Ar/C_2H_6 (90:10)	1 atm	- 1350 V	- 1000 V	- 650 V	- 400 V	332 ± 4 μm	246 ± 3 μm/ $\sqrt{\text{cm}}$
Ar/C_2H_6 (90:10)	2 atm	- 1570 V	- 1110 V	- 760 V	- 400 V	302 ± 10 μm	204 ± 6 μm/ $\sqrt{\text{cm}}$
$Ar/CF_4/isoC_4H_{10}$ (54:40:6)	1 atm	- 1630 V	- 1130 V	- 780 V	- 400 V	379 ± 8 μm	147 ± 8 μm/ $\sqrt{\text{cm}}$
$Ar/CF_4/isoC_4H_{10}$ (54:40:6)	1.4 atm	- 1810 V	- 1200 V	- 850 V	- 400 V	330 ± 4 μm	128 ± 4 μm/ $\sqrt{\text{cm}}$

Table 2: Efficiency, ARM, and SPD of the ETCC

Gas	Pressure	Efficiency	ARM (FWHM)	SPD (FWHM)
Ar/C_2H_6 (90:10)	1 atm	1.81×10^{-5}	10.4 ± 0.7°	114.8 ± 2.2°
Ar/C_2H_6 (90:10)	2 atm	3.55×10^{-5}	11.1 ± 0.4°	105.1 ± 1.2°
$Ar/CF_4/isoC_4H_{10}$ (54:40:6)	1 atm	2.44×10^{-5}	11.7 ± 0.4°	117.9 ± 1.6°
$Ar/CF_4/isoC_4H_{10}$ (54:40:6)	1.4 atm	3.51×10^{-5}	11.2 ± 0.3°	119.1 ± 1.1°

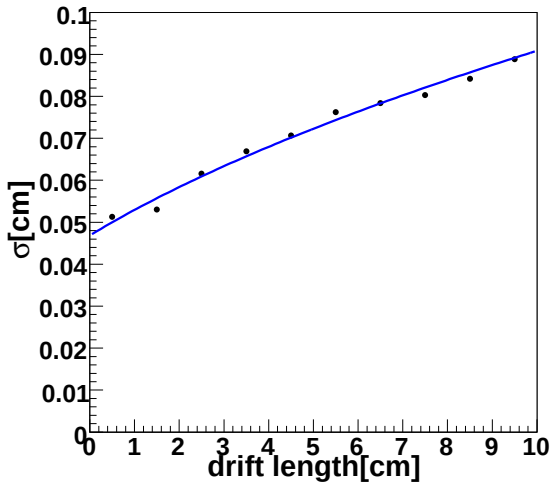

Figure 6: Position resolution in Ar/C_2H_6 (90:10) at 1 atm.

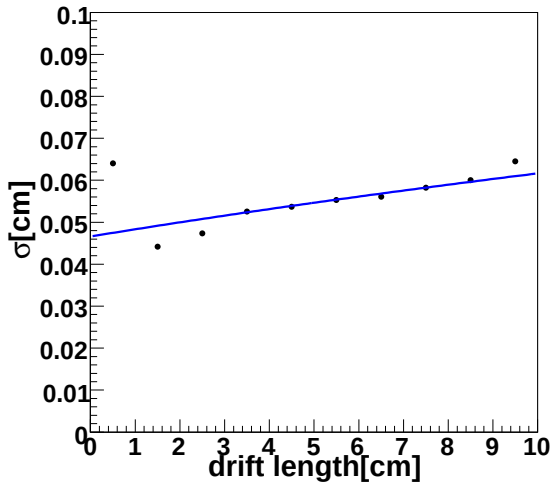

Figure 7: Position resolution in $Ar/CF_4/isoC_4H_{10}$ (54:40:6) at 1.4 atm.

1.4 atm were similar to those obtained with Ar/C_2H_6 (90:10) at 1 atm. However, these were about 2 degrees worse than the best records reached with our prototype. But, if we could recover the good position resolution and energy resolution of the μTPC, we would get resolutions similar to the prototype.

4. Summary

In order to improve the efficiency of the ETCC, we have optimized the gas mixture and the pressure in the μTPC. The gas mixture containing the highest fraction of CF_4 gas with a steady gas gain of ~ 20,000 is $Ar/CF_4/isoC_4H_{10}$ (54:40:6). The diffusion constant of $Ar/CF_4/isoC_4H_{10}$ (54:40:6) is about 2 times better than that of Ar/C_2H_6 (90:10), leading to an improved position resolution. The efficiency for the ETCC, using $Ar/CF_4/isoC_4H_{10}$ (54:40:6) at 1.4 atm, is 2 times higher than that with Ar/C_2H_6 (90:10) at 1 atm, and the ARMs are comparable (~ 11° at 356 keV (FWHM)). However, the efficiency in $Ar/CF_4/isoC_4H_{10}$ (54:40:6) at 1.4 atm is similar to the one in Ar/C_2H_6 (90:10) at 2 atm. If we could optimize the gas mixture at a higher pressure than 1.4 atm, the efficiency would become higher. It is also expected that the efficiency of the ETCC would become higher when we use $Ar/CF_4/isoC_4H_{10}$ (54:40:6) in a large-size ETCC with a detection volume of $30 \times 30 \times 30$ cm^3.

Acknowledgments

This work is supported by a Grant-in-Aid in Scientific Research from the Japan Ministry of Education, Science, Sports and Technology, "Ground Research Announcement for Space Utilization" promoted by Japan Space Forum, SENTAN of the Japan Science and Technology Agency, and the Global COE Program "The Next Generation of Physics, Spun from Universality and Emergence".

References

[1] T. Tanimori, et al., Astron. Rev. 48 (2004) 263.
[2] F. Sauli, Nucl. Instr. and Meth. A 386 (1997) 531.
[3] A. Ochi, et al., Nucl. Instr. and Meth. A 471 (2001) 264.
[4] S. Kabuki, et al., Nucl. Instr. and Meth. A 580 (2007) 1031.
[5] S. Kurosawa, et al., IEEE Trans. Nucl. Sci. 56 (2009) 3779.
[6] K. Ueno, et al., Nucl. Instr. and Meth. A 591 (2008) 268.
[7] H. Sekiya, et al., Nucl. Instr. and Meth. A 563 (2006) 49.
[8] S. Kurosawa, et al., Nucl. Instr. and Meth. A, in press.
[9] S. Kabuki, et al., IEEE Nucl. Sci. Symp. Conf. Rec. (2008) 3937.
[10] A. Takada, et al., J. Phys. Soc. Jpn. 78 (2009) Suppl. A, pp. 161.
[11] T. Tamagawa, et al., Nucl. Instr. and Meth. A 608 (2009) 390.
[12] H. Kubo, et al., Nucl. Instr. and Meth. A 513 (2003) 94.
[13] S.F. Biagi, Nucl. Instr. and Meth. A 421 (1999) 234.